Published in final edited form as:
*Polymer (Guildf)*. 2014 August 5; 55(16): 3894–3904. doi:10.1016/j.polymer.2014.05.045.

# Time Dependence of Material Properties of Polyethylene Glycol Hydrogels Chain Extended with Short Hydroxy Acid Segments

**Danial Barati**, **Seyedsina Moeinzadeh**, **Ozan Karaman**, and **Esmaiel Jabbari**
Biomimetic Materials and Tissue Engineering Laboratory, Department of Chemical Engineering, University of South Carolina, Columbia, SC 29208, USA

## Abstract

The objective of this work was to investigate the effect of chemical composition and segment number (n) on gelation, stiffness, and degradation of hydroxy acid-chain-extended star polyethylene glycol acrylate (SPEXA) gels. The hydroxy acids included glycolide (G,), L-lactide (L), p-dioxanone (D) and -caprolactone (C). Chain-extension generated water soluble macromers with faster gelation rates, lower sol fractions, higher compressive moduli, and a wide-ranging degradation times when crosslinked into a hydrogel. SPEGA gels with the highest fraction of inter-molecular crosslinks had the most increase in compressive modulus with n whereas SPELA and SPECA had the lowest increase in modulus. SPEXA gels exhibited a wide range of degradation times from a few days for SPEGA to a few weeks for SPELA, a few months for SPEDA, and many months for SPECA. Marrow stromal cells and endothelial progenitor cells had the highest expression of vasculogenic markers when co-encapsulated in the faster degrading SPELA gel.

### Keywords

hydrogel chain extension; hydroxy acids; cell encapsulation

## Introduction

The delivery of stem cells in a supportive carrier is an exciting approach to the regeneration of damaged biological tissues. In that approach the carrier acts as a temporary matrix for immobilization of the cells in the site of regeneration which is gradually displaced with the extracellular matrix (ECM) secreted by the encapsulated cells. The temporary matrix should provide a three-dimensional hydrophilic and aqueous environment to support complex cell-matrix interactions but gradually degrade concurrent with ECM formation [1-4]. Due to their high water content, hydrogels have high permeability to oxygen and nutrients required for



**Corresponding author:** Esmaiel Jabbari, Ph.D. Associate Professor of Chemical and Biomedical Engineering Swearingen Engineering Center, Rm 2C11 University of South Carolina Columbia, SC 29208 Tel: (803) 777-8022 Fax: (803) 777-0973 jabbari@mailbox.sc.edu.

cell survival and function [5]. Further, cell-loaded hydrogel precursor solutions can be injected and gelled *in situ* to fill defects with irregular shapes. Inter-diffusion of hydrogel chains to tissues proximal to the defect leads to superior integration of the carrier with the surrounding tissue after gelation [6].

Due to their non-immunogenic and inert nature, polyethylene glycol (PEG) hydrogels are very attractive as a matrix for stem cell delivery to the site of regeneration [6-8]. Adhesion and differentiation of cells encapsulated in PEG gels can be tuned by conjugation with integrin-binding ligands and morphogenetic peptides, respectively [9-11]. A major drawback to the widespread use of PEG gels is their persistence in the site of regeneration. Although copolymerization of PEG macromers with resorbable monomers can be used to impart degradability to the hydrogel [12, 13], degradability is offset by lower macromer solubility in aqueous solution for cell encapsulation and low gel stiffness [14, 15].

Recently, we reported that the extension of star PEG macromers with very short hydroxy acid segments imparted degradability to the hydrogel without changing macromer solubility in aqueous solution and hydrogel stiffness [14, 16]. Molecular dynamic simulations demonstrated the formation of micellar structures (<3 nm in size) that dramatically increased the local concentration of reactive groups, leading to a potentially higher modulus with little change in the overall water content of the hydrogel [17]. Further, human MSCs encapsulated in the high-stiffness, relatively slow-degrading lactide-chain-extended PEG hydrogels had higher extent of differentiation to the osteogenic lineage than those encapsulated in non-degradable PEG gels [16].

It is well-established that the fate of encapsulated cells is determined by the physical and mechanical properties of their microenvironment including degradation rate and stiffness. For example, marrow stem cells (MSCs) encapsulated in a non-degradable hyaluronic acid (HA) gel had a rounded morphology and underwent adipogenic differentiation whereas those MSCs encapsulated in a degradable HA gel spread and differentiated to the osteogenic lineage [18]. Similarly, the C2C12 mouse myoblast cells encapsulated in a soft degradable alginate gel (13 kPa modulus) had a higher extent of differentiation to myotubes and lower proliferation than those encapsulated in a non-degradable stiff gel (45 kPa modulus) [19]. Tissue engineered constructs often times require multiphase hydrogels with different but complementary microenvironments. For example, osteogenic differentiation of MSCs requires a supporting matrix with high compressive modulus and slow degradation [20] whereas vasculogenic differentiation of progenitor endothelial cells necessitates a low modulus, relatively fast-degrading matrix [21, 22]. Therefore, there is a need to develop synthetic hydrogels with tunable degradation and stiffness for wide-ranging applications in regenerative medicine.

The objective of this work was to investigate the effect of chemical composition and length of the hydroxy acid in hydroxy acid-chain-extended star PEG acrylate macromer on gelation characteristics, water content, compressive modulus, and degradation of the hydrogels with incubation time. The hydroxy acid monomers included the least hydrophobic glycolide, L-lactide, p-dioxanone, and the most hydrophobic -caprolactone. The findings of this work demonstrate that chain extension of star PEG macromers with the above hydroxy acids

produces hydrogels with a wide range of physical and mechanical properties to serve as cell carriers in regenerative medicine from the compliant vascular tissue to the stiff bone tissue.

## Experimental

### 1. Materials

Lactide, glycolide and p-dioxanone monomers (L, G, D; >99.5% purity) were purchased from Ortec (Easley, SC) and -Caprolactone (C) was purchased from Alfa Aesar (UK). The monomers were dried under vacuum at 40°C for at least 12 h prior to polymerization. Calcium hydride, tetrahydrofuran (THF), deuterated chloroform (99.8% deuterated), trimethylsilane (TMS), triethylamine (TEA), tin(II) 2-ethylhexanoate (TOC), acryloyl chloride, and dimethylsulfoxide (DMSO) were purchased from Sigma-Aldrich (St. Louis, MO). 4-arm PEG (SPEG, $M_w$=5000) was purchased from Sigma-Aldrich. The protected amino acids and Rink Amide NovaGel resin for the synthesis of acrylamide-terminated GRGD peptide were purchased from EMD Biosciences (San Diego, CA). Dichloromethane (DCM, Acros Organics, Pittsburg, PA) was dried by distillation over calcium hydride. Diethyl ether and hexane were obtained from VWR (Bristol, CT). The dialysis tube (molecular weight cutoff 3.5 kDa) was purchased from Spectrum Laboratories (Rancho Dominquez, CA). EBM-2 medium, vascular endothelial growth factor (VEGF), human fibroblast growth factor-B (hFGF-B), $R^3$-insulin-like growth factor ($R^3$-IGF-1), human epidermal growth factor (hEGF), ascorbic acid hydrocortisone, gentamycin, and amphotericin-B were purchased from Lonza (Hopkinton, MA). Dulbecco's Modified Eagle Medium (DMEM; 4.5 g/L glucose with L-glutamine without sodium pyruvate) was purchased from Mediatech (Herndon, VA). Medium 199 with L-glutamine was purchased from Sigma-Aldrich. 3-(4,5-dimethyl-2-thiazolyl)-2,5-diphenyl-2H-tetrazolium bromide (MTT) was purchased from Calbiochem (EMD Millipore, Billerica, MA).

### 2. Macromer synthesis

The 4-arm poly(ethylene glycol) (SPEG) macromer was extended with D, C, G and L monomers via Ring Opening Polymerization (ROP) to synthesize SPED, SPEC, SPEG and SPEL macromers, respectively, as we previously described [15, 16]. Briefly, for the synthesis of SPEC, SPEG and SPEL macromers, the PEG and monomer were added to a three-neck reaction flask equipped with a stirrer and immersed in an oil bath. The feed molar ratio of the PEG to monomer was based on the desired length of the degradable segment on each macromer arm. Next, the flask was heated to 120°C under nitrogen flow and maintained at that temperature for one hour before the addition of TOC catalyst. The polymerization reaction was allowed to proceed for 12 h at 140°C, 160°C and 140°C for SPEC, SPEG and SPEL, respectively. For the synthesis of SPED, the PEG and catalyst mixture was heated to 130°C to remove moisture, cooled to 85°C for addition of D monomer, and the reaction was allowed to proceed for 48 h at 85°C. The reaction product was precipitated in ice-cold hexane to remove the unreacted monomer and catalyst.

Next, the hydroxy acid chain-extended PEG macromer was functionalized with acrylate groups. The product of the first reaction was dissolved in DCM and dried by azeotropic distillation from toluene. In a reaction flask placed in an ice bath, equimolar amounts of

acryloyl chloride (Ac) and triethylamine (TEA) were added dropwise to the solution of chain-extended macromer in DCM and the reaction was allowed to proceed for 12 h under dry nitrogen atmosphere. After the reaction, the product was dried by rotary evaporation and dissolved in ethyl acetate to precipitate the triethylamine hydrochloride salt. The product was then dried and precipitated in ice-cold ethyl ether twice. Next, the product was dissolved in DMSO and dialyzed against water (3.5 kDa MW cutoff Spectro/Por dialysis membrane) to remove any remaining impurities. Acrylate-terminated SPEXA macromers, where "X" is G, L, D or C, were dried in vacuum to remove the residual solvent and stored at –20°C. The notations nXa is used to identify the number of degradable monomers on SPEXA macromers, where X is type of the hydroxy acid monomer and "a" is the number of hydroxy acid monomers per macromer.

### 3. Macromer characterization

The chemical structure of the macromers was characterized by a Varian Mercury-300 HNMR (Varian, Palo Alto, CA) at ambient conditions with a resolution of 0.17 Hz [23]. The samples were dissolved in deuterated chloroform at a concentration of 50 mg/mL and 1% TMS v/v was the internal standard.

### 4. Macromer gelation and rheological characterization

The SPEXA macromers were crosslinked in aqueous solution by ultraviolet-initiated polymerization as we described previously [16]. Briefly, the photoinitiator solution (Irgacure 2959; CIBA, Tarrytown, NY) was mixed with the macromer solution by vortexing for 5 min at 50°C. Based on our previous results [14], the initiator concentration of 0.75 wt% (based on the macromer weight) was used in the hydrogel precursor solution to minimize cell toxicity and optimize the extent of gelation. To measure compressive modulus of the gels, the hydrogel precursor solutions were degassed and transferred to a polytetrafluoroethylene (PTFE) mold (5 cm × 3 cm × 750 μm), covered with a transparent glass plate and fastened with clips. Next, the samples were irradiated with a BLAK-RAY 100W mercury, long-wavelength (365 nm) UV lamp (B100-AP; UVP, Upland, CA) for 10 min. Disk-shaped samples were cut from the gel using an 8-mm cork borer and loaded on the Peltier plate of the rheometer (TA Instruments, New Castle, DE) and subjected to a uniaxial compressive force at a displacement rate of 7.5 mm/s. The slope of the linear fit to the stress–strain curve for 5%–10% strain was taken as the elastic modulus (E) of the gels, as we previously described [24].

To measure gelation time, the hydrogel precursor solution was directly loaded on the peltier plate of an AR-2000 rheometer (TA Instruments, New Castle, DE) and irradiated at a distance of 10 cm from the sample. A sinusoidal shear strain with frequency of 1 Hz and amplitude of 1% was exerted on the sample and the storage ($G'$) and loss moduli ($G''$) were recorded with time. The time at which $G' = G''$ was recorded as the gelation time, as we previously described [15].

### 5. Measurement of swelling ratio, sol fraction and mass loss

Disk shape hydrogel samples with a diameter of 8 mm and a thickness of 750 μm were dried at ambient conditions for 12 h followed by drying in vacuum for 1 h at 40°C. After drying,

the dry weights ($w_i$) were recorded. Next, the dry samples were swollen in DI water for 24 h at 37°C with a change of swelling medium every 6 hours. After swelling, the surface water was removed and the swollen weights ($w_s$) were measured. Then, the swollen samples were dried as described above and the dry weights ($w_d$) were recorded. The swelling ratio (Q) and sol fraction (S) were calculated from the dry and swollen weights using previously described equations [25]. To measure mass loss, the dried samples disk were incubated in 5 mL basal medium without fetal bovine [16] serum at 37°C under mild agitation. At each time point, samples were washed with DI water to remove excess electrolytes, dried under vacuum, and the dry sample weights were measured and compared with the initial dry weights to determine fractional mass remaining as previously described [14].

## 6. Cell isolation and culture

MSCs were isolated from the bone marrow of young adult male Wistar rats (6-8 weeks) as we previously described [10, 23, 26]. Cell isolations were performed under a protocol approved by the Institutional Animal Care and Use Committee of the University of South Carolina. The marrow of the removed tibias and femurs were flushed with cell isolation medium [23], the cell suspension was centrifuged at 200g for 5 min. Next, the cell pellets were re-suspended in primary medium (DMEM supplemented with 10% FBS [23]), aliquoted into tissue culture flasks and maintained in a humidified 5% $CO_2$ incubator at 37°C. The medium was replaced with fresh medium at 3 and 7 days to remove unattached cells. The enzymatically lifted MSCs were used for cell culture experiments. To isolate endothelial progenitor cells (EPCs) from the rat bone marrow, the marrow cavity of the tibias and femurs were flushed with Medium 199 supplemented with 20% FBS, 1% Pen/Strep and 22.5 μg/ml heparin [27, 28]. The cell suspension was centrifuged at 200g for 5 min and the cell pellet was re-suspended in Medium-199 and plated on rat-derived fibronectin-coated 6-well plates (1μg/mL). After 24h, the non-adherent cells in the medium were recovered and transferred to a new fibronectin-coated plate. This procedure was repeated to remove rapidly adherent hematopoietic cells or mature endothelial cells in the aspirate [27, 28]. Only the non-adherent cell population was harvested after 48 h and used for cell culture experiments.

The MSC/EPCs (1:1 cell ratio) were encapsulated in PEGDA, nL6.4, nD6.8, and nC7.2 hydrogels. MSCs in the co-culture act as pericytes to facilitate maturation and stabilization of tubular structures formed by multi-cellular assembly of EPCs [29, 30]. Recent reports indicate that the extent of vasculogenic differentiation of EPCs shows a decreasing trend with increasing matrix stiffness [30]. Therefore, the lowest compressive modulus of 5 kPa attainable with SPEXA gels was used in all cell encapsulation experiments. The SPEGA gel was not used for cell encapsulation because the gel completely degraded in <3 days incubation in vsaculogenic medium.

To facilitate cell adhesion to the hydrogel matrix, acrylamide-terminated GRGD peptide (Ac-GRGD) was synthesized on Rink Amide NovaGel resin and characterized by mass spectrometry as we previously described [11]. For cell encapsulation, MSCs ($5 \times 10^6$ cells/mL) and EPCs ($5 \times 10^6$ cells/mL) were suspended in the sterile hydrogel precursor solution composed of SPEXA macromer, Ac-GRGD (2 wt% of the macromer), and

photoinitiator (0.75% of the macromer) in phosphate buffer saline (PBS) as we previously described [14]. The cell suspension was injected between two sterile glass slides and crosslinked by exposure to UV light for 200 sec, the minimum exposure time for the gel to reach its plateau modulus. After gelation, the samples were incubated in basal medium for 1 h with two medium changes to remove the unreacted macromers. Next, the medium was replaced with complete vasculogenic medium (EBM-2 medium containing VEGF, human hFGF-b, IGF-1, human EGF, ascorbic acid, hydrocortisone, gentamycin, and amphotericin B) and cultured in a humidified 5% $CO_2$ incubator for up to 12 days as we previously described [27].

### 7. Biochemical and mRNA analysis

For measurement of cell viability, at each time point (1, 3 and 7 days), the gel samples were placed in a 24 well plate and 500 μL of serum-free DMEM containing 0.5 mg/mL of MTT was added to each well. The MMT assay is based on the conversion of MTT into insoluble formazan crystals by oxidoreductase enzymes in the mitochondria of the cell. After 3 h incubation at 37 C, the medium was replaced with 500 μL of DMSO for dissolution of the formazan crystals. The plate was incubated for 4 h in dark and the absorbance was measured at the peak wavelength of 560 nm with a plate reader (Synergy HT, Bio-Tek, Winooski, VT). Results were expressed as relative cell viability compared to day 1 for the control PEGDA gel. For DNA content, collagen content and mRNA measurements, at each time point (3, 6, 12 days), gel samples were washed with serum-free DMEM for 8 h to remove serum components, washed with PBS, lysed with lysis buffer (10 mM tris and 2% triton) and sonicated. After centrifugation, the supernatant was used for measurement of total DNA and collagen content. The double-stranded DNA content of the samples was determined using a Quant-it PicoGreen assay (Invitrogen, Carlsbad, CA) at emission and excitation wavelengths of 485 and 528 nm, respectively, according to the manufacturer's instructions as described [10]. Total collagen content was measured with a Sircol collagen assay based on selective binding of G-X-Y amino acid sequence of collagen to Sircol dye at absorbance wavelength of 555 nm, according to manufacturer's instructions as described [16, 31]. For RNA analysis, at each time point, total cellular RNA was isolated using TRIzol (Invitrogen, Carlsbad, CA) plus RNeasy Mini-Kit (Qiagen, Valencia, CA) according to the manufacturer's instructions as described [16]. A 1 μg of the extracted RNA was subjected to cDNA conversion using the Reverse Transcription System (Promega, Madison, WI). Primers for real-time PCR (RT-qPCR) analysis were designed and selected using the Primer3 web-based software as described elsewhere [32]. RT-qPCR was performed to analyze the differential expression of PECAM-1, vWF and VE-cadherin genes with SYBR green RealMasterMix (Eppendorf, Hamburg, Germany) using a Bio-Rad iCycler machine (Bio-Rad, Hercules, CA) and iCycler optical interface version 2.3 software. The forward and reverse primers (synthesized by Integrated DNA technologies, Coralville, IA) were as follows: PECAM-1: forward 5`-CGAAATCTAGGCCTCAGC AC-3` and reverse 5`-CTTTTTGTCCAC GGTCACCT-3`; vWF: forward 5`-GCTCCAGCA AGTTGAAGACC-3` and reverse 5`-GCA AGTCACTGTGTGGCACT–3`; VE-cadherin: forward 5`-GCACCAGTTTGGCCAATATA-3` and reverse 5`-GGGTTTTTGCATAATAAGCAGG-3`; S16: forward 5'-AGTCTTCGGACG CAAGAAAA-3' and reverse 5'-AGCCACCAGAGCTTTTGAGA-3' [10, 33]. The

expression ratio of the gene of interest to that of S16 housekeeping gene was determined using the Pfaffl model and normalized to the first time point [34].

### 8. Statistical analysis

Data are expressed as means ± standard deviation. All experiments were done in triplicate. Significant differences between groups were evaluated using a two-way ANOVA with replication test followed by a two-tailed Student's t-test. A value of $p < 0.05$ was considered statistically significant.

## Results and Discussion

### 1. Macromer characterization

The average number of degradable monomers as well as the number of acrylate groups per macromer arm was measured by $^1$H-NMR spectrometry as we previously described [14]. The average number of degradable monomers per macromer arm was determined from the ratio of the shifts centered at 1.4, 1.7, 2.3 and 4.1 ppm ( -caprolactone hydrogens), 3.7, 4.2 and 4.4 ppm (p-dioxanone hydrogens), 1.6 and 5.2 ppm (L-lactide hydrogens) and 4.8-4.9 ppm (glycolide hydrogens) to those at 3.6 and 4.3 ppm (PEG hydrogens). The average number of acrylate groups per macromer arm was determined from the ratio of the shifts between 5.85 and 6.55 ppm (acrylate hydrogens) to those at 3.6 and 4.2 ppm (PEG hydrogens). The average number of monomers and acrylate groups incorporated on each arm of the macromers and number average molecular weight ($\overline{M_n}$) of the SPEXA macromers are shown in Table 1. The number of monomers per end group varied from 0.7 to 2.8 for SPECA, 0.6 to 2.9 for SPEDA, 0.8 to 2.9 for SPELA and 0.7 to 2.8 for SPEGA as the monomer to PEG feed molar ratio was increased from 5 to 15. Further, the average number of acrylates per SPEXA end group ranged from 0.71 to 0.87.

### 2. Effect of acrylate concentration on SPEXA gelation kinetics

The effect of acrylate concentration in the precursor solution, which was varied by changing the macromer concentration (Table 1), on compressive modulus, gelation time, swelling ratio and sol fraction of SPECA nC7.2, SPEDA nD6.8, SPEGA nG6.4 and SPELA nL6.4 macromers is shown in Figures 2a to 2d, respectively. The compressive modulus of SPECA, SPEDA, SPEGA and SPELA gels increased from 5 kPa to 480, 560, 710 and 460 kPa, respectively, with increasing acrylate concentration from 0.02 to 0.13 mol/L (Figure 2a). Gelation times of SPEDA and SPEGA hydrogels decreased from 140 to 63 sec and 128 to 60s, respectively, with increasing acrylate concentration from 0.02 to 0.13 mol/L (Figure 2b). Gelation times of SPECA and SPELA gels ranged from 77 to 30 sec and 64 to 28 sec, respectively, which were significantly lower than those of SPEDA and SPEGA. The SPECA and SPEGA gels had the lowest and highest swelling ratio, respectively, for all acrylate concentrations (Figure 2c). The swelling ratio of SPECA and SPEGA gels decreased from 710 to 300% and from 830 to 430%, respectively, as the acrylate concentration increased from 0.02 to 0.13 mol/Lit. The swelling ratio of SPEDA and SPELA gels was between those of SPECA and SPEGA and decreased from 750 and 730 to 340%, respectively, with increasing acrylate concentration from 0.02 to 0.13 mol/L. The sol fraction of SPECA, SPEDA and SPELA gels decreased from 13 to 6%, 14 to 5.5% and 11 to 5%, respectively,

with increasing acrylate concentration from 0.02 to 0.13 mol/L (Figure 2D). The sol fraction of SPEGA gel was significantly lower than the other gels and ranged between 8 to 2% in the acrylate concentration range of 0.02 to 0.13 mol/L. According to the theory of rubber elasticity, the elastic modulus of a crosslinked network is [35]

$$\mathrm{E}=v_{\mathrm{E}}RT \quad (1)$$

Where $V_E$ , R and T are the density of elastically active chains, gas constant and absolute temperature, respectively. The density of acrylate-acrylate bonds increased with increasing the acrylate concentration in the precursor solution. Furthermore, the probability of reaction between two acrylates on the same macromer (intra-molecular acrylates) decreased with increasing the acrylate concentration. It is well established that intra-molecular reactions lead to the formation of loops that do not contribute to the network elasticity [25, 36]. As a result of that the compressive modulus of SPEXA gels increased monotonically with increasing acrylate concentration (Figure 2a). The difference between the elastic modulus of SPEXA gels at a given acrylate concentration is related to the chemical composition of degradable monomers. We have recently demonstrated that SPEXA macromers aggregate and form micellar structures in the hydrogel precursor solution [16, 17] with the hydrophobic acrylate-terminated degradable segments and the hydrophilic PEG segments forming the core and corona of the micelles, respectively. Further, the propensity for micelle formation and micelle size increased with increasing hydrophobicity of the degradable segment from G to D, L and C [16]. Furthermore, the fraction of acrylate groups in the aqueous solution free from the micelle core increased from SPECA to SPELA and SPEDA, with SPEGA having the highest fraction of free acrylates [16]. As a result, a major part of the crosslinking reaction occurred in the aqueous phase for the less hydrophobic SPEGA and SPEDA macromers which lead to the formation of a uniform network at the molecular scale and longer gelation times (Figure 2b). On the contrary, the crosslinking reaction occurred predominantly in the micellar structures for the more hydrophobic SPELA and SPECA macromers with higher local concentrations of acrylates, which lead to a faster crosslinking and shorter gelation times (Figure 2b). The diffusivity of unreacted acrylates was limited in the crosslinked hydrophobic domains which reduced the extent of crosslinking in the micelles for SPELA and SPECA gels. Consequently, the gelation times of SPEGA and SPEDA precursor solutions (Figure 2b) and compressive modulus of their gels (Figure 2a) were higher than those of SPELA and SPECA. The decrease in swelling ratio of SPEXA gels with acrylate concentration in Figure 2c was related to the increase in crosslink density at higher acrylate concentrations. The water content of a hydrogel is controlled by two opposing free energies, namely free energy of mixing and elastic free energy. The free energy of mixing tends to increase the water content of the gel by attractive interactions between water molecules and the network chains [37]. The elastic free energy on the other hand tends to decrease the water content of the gel due to the extension of random coil chain conformation. Hydrophobicity of the macromers affects the free energy of mixing whereas crosslink density affects the elastic free energy. Therefore, at a given macromer concentration, the swelling ratio of SEPXA gels decreased with increasing macromer hydrophobicity due to the decrease in free energy of mixing (Figure 2c). Further, the

swelling ratio of the gels decreased with increasing acrylate concentration due to the formation of a network with higher crosslink density.

### 3. Effect of hydrophobic monomers per macromer arm on SPEXA gelation kinetics

The effect of the number of degradable hydrophobic monomers per macromer arm (n) on compressive modulus, gelation time, swelling ratio and sol faction of SPECA, SPEDA, SPEGA and SPELA hydrogels at constant acrylate concentration of 0.1 (mol/L) is shown in Figures 3a-d, respectively. The compressive modulus of SPELA, SPECA, SPEDA and SPEGA gels increased significantly from 330 to 390, 420, 500 and 620 kPa, respectively, as the number of monomers per end group (n/4) was increased from 0 to 2.9 (2.8 for C). The aforementioned increase was related to a change in the structure of the gel at the molecular scale as we previously described [16, 17]. The reactive acrylates are uniformly distributed in aqueous solution in the absence of chain extension of PEG with hydrophobic segments [16]. With hydroxy acid chain extension, micellar structures are formed which increase the local concentration of acrylates in the micellar domains with increasing n at constant bulk acrylate concentration [16]. The probability of intra-molecular reaction for a pendant double bond (Ψ) in the free radical crosslinking reaction of multi-functional macromers is [38]

$$\psi = 1 - exp\left(\frac{-3}{4\pi N_A [DB] r_0 l^2}\right) \quad (2)$$

Where [DB] is the concentration of double bonds, $r_0$ is the average distance between double bonds on a macromer, l is the statistical length of a repeating unit and $N_A$ is the Avogadro's number. According to equation 2, the extent of cyclization decreased with increasing n due to the increase in local acrylate concentration in the micellar structures and the increase in end-to-end distance of the macromers. The compressive modulus of SPEXA gels increased with increasing n (Figure 3a) because the number of intra-molecular loops that did not contribute to network elasticity was reduced with increasing n. There was an increasing trend in compressive modulus of SPEXA gels with SPEGA and SPELA as the stiffest and softest gels, respectively, at a given n value. Further, the gelation time of SPEDA and SPEGA decreased from 150 to 64 and 61 sec when the number of monomers per end group increased from 0 to 2.9 and 2.8, respectively, whereas the gelation time of SPECA and SPELA decreased from 150 to 34 and 38 sec with increasing the number of monomers per end group from 0 to 2.8 and 2.9 (Figure 3b). The gelation times of SPECA and SPELA was significantly lower than those of SPEGA or SPEDA for all n values. The difference in compressive modulus of SPEXA gels at the same n can be attributed to differences in diffusivity and residence time of the reactive acrylates in the micellar structures. The residence time of the acrylates in the micelles' core was directly correlated to the effective interfacial tension between the chain ends and water (γ) [39, 40] in which γ increased with hydrophobicity of the monomers from G to D, L and C. Therefore, the residence time of the acrylates in SPELA and SPECA was higher than those of SPEDA and SPEGA which lead to the higher entrapment of reactive acrylates in the crosslinked micellar domains and faster gelation times for SPELA and SPECA (Figure 3b). The lower residence time of the acrylates in SPEGA and SPEDA led to higher diffusivity of the acrylates, slower but more uniform

crosslinking throughout the solution, resulting in the higher compressive modulus of the gels.

The swelling ratio of SPECA, SPELA, SPEDA and SPEGA hydrogels decreased from 490 to 350, 390, 370 and 430%, respectively, with increasing the number of monomers per end group from 0 to 2.9 (2.8 for X= G, C). SPECA and SPEGA hydrogels had the lowest and highest swelling ratios, respectively, for all n values (Figure 3c). The sol fraction of SPECA, SPELA, SPEDA and SPEGA varied from 9.6 to 6.4, 6.3, 7.2 and 3.1%, respectively, when the number of monomers per end group was increased from 0 to 2.9 (2.8 for X= G, C). The sol fraction of SPEGA was significantly lower than the other three gels for all n values (Figure 3d).

### 4. Effect of hydrophobic monomers per macromer arm on SPEXA gel degradation

The mass remaining for SPEXA gels after 1, 5, 10, 20, 30 and 40 days of incubation in PBS is shown in Figure 4. The mass loss of SPEGA hydrogels increased from 8 to 19, 31 and 46% with increasing n from 2.8 to 4.8, 6.4 and 11.2, respectively, after one day incubation. The SPEGA gels with n of 6.4 and 11.2 completely degraded after 5 days incubation. Since the SPEGA had the highest water content among SPEXA gels and each G monomer had two ester groups, SPEGA gels had the fastest mass loss with incubation on the time scale of a week. On the other hand, the remaining mass of SPELA gels did not significantly change after 1 day incubation. The remaining mass of SPELA gels with n of 7.2 and 11.4 after 5 days incubation decreased to 84 and 71%, respectively; it decreased to 69 and 27% after 20 days and the gels completely degraded after 30 and 40 days. The remaining mass of SPELA gels with n of 2.7 and 4.8 after 40 days incubation was 51 and 45%, respectively. Since SPEDA and SPECA gels had the lowest water content and each D/C monomer had one ester group [16], these gels had the slowest mass loss among SPEXA gels and their degradation was not significantly affected by the length of the hydrophobic segment; SPEDA and SPECA mass remaining after 20 days ranged from 76 to 70% and 92 to 87%, respectively, and they ranged from 61 to 69% and 80 to 89% after 40 days. Due to their higher water content (Figure 3c), mass loss of SPEDA gels was faster than SPECA.

### 5. Effect of hydrophobic monomers per macromer arm on SPEXA swelling ratio

The effect of number of monomers per end group of the macromer on swelling ratio of SPECA, SPEDA, SPELA and SPEGA hydrogels with incubation time is shown in Figures 5a-d, respectively. The swelling of SPECA and SPEDA hydrogels reached a plateau with incubation time for all n values (Figure 5a,b). The swelling ratio of SPEDA gel increased with decreasing n from 11.6 to 6.8 for all incubation times but swelling was unaffected for $n<6.8$ (Figure 5b). The swelling ratio of SPELA gels decreased with increasing n in the first 7 days of incubation. However, that trend was reversed after 7 days and swelling ratio increased with increasing n (Figure 5c). Due to their high water content, SPELA gels with n of 7.2 and 11.4 disintegrated after 14 and 20 days, respectively. The SPELA gel with n of 11.4 rapidly swelled from 360 to 660% from day zero to 14 whereas those with n of 7.2, 4.8 and 2.7 swelled to 620, 600 and 580%, respectively (Figure 5c). The inversion in SPELA gel swelling was attributed to a higher increase in hydrophilicity of the gel with mass loss as n was increased. Since mass loss was proportional to the hydrophobic segment length and

crosslink density decreased with mass loss [41], there was a faster decrease in crosslink density with incubation time for SPELA gels with higher n, leading to higher swelling ratios for those gels with higher n. The nG11.2 and nG6.4 SPEGA gels disintegrated one day after incubation due to high swelling ratios whereas the nG2.8 and nG4.8 gels disintegrated after 4 days. The swelling ratios of SPEGA gels initially increased with increasing n from 2.8 to 6.4 in the first day of incubation and then decreased with increasing n from 6.4 to 11.2 (Figure 5d).

## 5. Effect of hydrophobic monomers per macromer arm on compressive modulus of SPEXA gels

The effect of number of hydrophobic monomers per macromer arm on compressive modulus of SPECA, SPEDA, SPELA and SPEGA gels with incubation time is shown in Figures 6a-d, respectively. The compressive modulus of SPEXA gels decreased with incubation time as the gel crosslink density decreased with mass loss. The initial compressive modulus of SPEXA gels increased with n for a given macromer concentration. Assuming a pseudo first order reaction for hydrolysis of SPEXA gels, the crosslink density should decay exponentially with time [42]. Based on the theory of rubber elasticity, the change in compressive modulus with incubation time should correlate with the rate constant for decay in crosslink density (k) as follows [43]

$$\mathrm{E} \sim \mathrm{e}^{\frac{6}{5}kt} \quad (3)$$

where t is incubation time. To compare crosslink decay for SPEXA gels, the k values were determined by fitting the data in Figure 6 [ln(E) versus time] to the linearized form of equation 3. The k value for SPECA gels increased from $2.9\times10^{-6}$ to $5.2\times10^{-6}$ $min^{-1}$ with increasing n from 2.8 to 11.2 which lead to a difference of 1.3 and 1.1-fold in compressive modulus between the two SPECA gels at day zero and after 42 days incubation, respectively (Figure 6a). The difference between the compressive modulus of nD11.6 and nD2.4 SPEDA gels was 1.5-fold and 1.1-fold at day zero and after 42 days incubation, respectively, which was attributed to the higher rate of crosslink decay in nD11.6 gel ($1.3\times10^{-5}$ $min^{-1}$) compared to nD2.4 gel ($7.5\times10^{-6}$ $min^{-1}$) (Figure 6b). Although the initial compressive modulus of SPELA gels increased with n, that trend was reversed after 3 days incubation (Figure 6c). For example, the compressive modulus of SPELA gels after 10 days incubation decreased from 235 to 220, 110 and 50 kPa as n increased from 2.7 to 4.8, 7.2 and 11.4. The rapid decline in compressive moduli of nL11.4 and nL7.2 compared to nL4.8 and nL2.7 gels was attributed to the significantly higher k values of nL11.4 ($1.2\times10^{-4}$ $min^{-1}$) and nL7.2 ($7.0\times10^{-5}$ $min^{-1}$) compared to those of nL4.8 ($1.2\times10^{-5}$ $min^{-1}$) and nL2.7 ($8.7\times10^{-6}$ $min^{-1}$). The k values of SPEGA gels increased from $5.4\times10^{-4}$ to $2.2\times10^{-3}$ $min^{-1}$ with increasing n from 2.8 to 11.2. The k value of the slowest degrading nC2.8 SPECA gel was three orders of magnitude lower than that of the fastest degrading nG11.2 SPEGA gel.

## 7. Effect of gel degradation on differentiation of endothelial progenitor cells

Early and rapid induction of vascularization in engineered cellular constructs after implantation is critical to successful regeneration of tissues [44]. The process of vascularization by endothelial cells requires a compliant and permissive microenvironment

[21]. In addition to those requirements, the generation of microvessels requires the presence of mural cells, vascular smooth muscle cells and pericytes, in the vicinity of endothelial cells for stabilization of microvessels [45]. In that respect, a mixture of MSCs and EPCs encapsulated in a methacrylated gelatin produced more stable microvessels compared to encapsulation of EPCs only [21] and the extent of microvessel formation was strongly dependent on the gel's compressive modulus and degradation. In this work, rat MSCs and EPCs were encapsulated in SPEXA gels with the same initial compressive modulus of 5 kPa and the effect of degradation on vasculogenic expression of the encapsulated MSC//EPCs was evaluated with incubation time. The SPEGA gel due to its complete degradation in <5 days was not used for cell encapsulation.

Figures 7a-f show the cell viability, DNA content, total collagen content, mRNA expression of vasculogenic markers PECAM-1, VE-cadherin, and von Willebrand Factor (vWF), respectively, for MSC/EPCs encapsulated in SPEXA gels with incubation time. The MSC/EPCs encapsulated in the non-degradable PEGDA gel was used as the control. Cell viability of SPEXA gels decreased slightly from day 1 to day 7. The MSC/EPCs encapsulated in the PEGDA gel had a slightly higher viability than those in SPEXA gels for all time points. However, the difference in cell viability between SPEXA and PEGDA gels was not statistically significant. A slight decrease in cell viability of SPELA gels with incubation time in the first 7 days was consistent with DNA content of the gels (Figure 7b). The slight decrease in cell viability of SPELA gels with incubation time was most likely related to its faster degradation compared to SPECA and SPEDA, which led to the higher extent of differentiation of MSC/EPCs in the SPELA gel. DNA content of the gels decreased as the cells differentiated to the vasculogenic lineage with incubation time, consistent with the previously reported results [21]. There was not a significant difference between DNA content of the cells encapsulated in SPEXA gels for all time points and those in the control PEGDA gel. Total collagen content of MSC/EPCs in the faster degrading SPELA gel after 12 days incubation was significantly higher than those in the other gels. The total collagen content of PEGDA, SPEDA, SPECA and SPELA gels was 59, 59, 67 and 94 μg/μg DNA, respectively, after 12 days incubation. This was consistent with previous reports that collagen secretion by encapsulated cells is related to the rate of matrix turnover [46, 47]. The slower degrading SPEDA and SPECA gels hindered collagen secretion by the encapsulated cells whereas the faster degrading SPELA gel enhanced collagen secretion. The platelet/endothelial cell adhesion molecule, PECAM-1 or CD31, is a transmembrane protein expressed early in vascular development [48]. VE-cadherin, a member of the cadherin family of adhesion receptors, is a constitutive marker of endothelial cells and plays an important role in early vascular assembly. Mature endothelial cells in the late phase of vasculogenesis secret vWF, a plasma protein that mediates platelet adhesion to damaged blood vessels and stabilizes blood coagulation factor VIII [49, 50]. PECAM-1, VE-cadherin and vWF mRNA expression of MSC/EPCs encapsulated in fast-degrading SPELA gel was significantly higher than those encapsulated in slow-degrading SPECA and SPEDA gels after 12 days incubation (Figures 7d-f), consistent with the results for total collagen secretion (Figure 7c). Further, the early marker PECAM-1 expression of the cells in SPELA gel after 6 days incubation was significantly higher than those in SPECA and SPEDA. After 12 days incubation, mRNA expression of PECAM-1, VE-cadherin and vWF for cells in

SPELA gel was 2.2, 1.7 and 2.1-fold higher than those cells encapsulated in non-degradable PEGDA gel.

In summary, the results demonstrate that chain extension of star PEG macromers with short hydroxy acid segments generates water soluble macromers that can be crosslinked into hydrogels with a wide range of degradation times from a few days for SPEGA to a few weeks for SPELA, a few months for SPEDA, and many months for SPECA. Further, SPEXA macromers can be blended to generate hydrogels with a wide range of decaying rates for modulus from complete disintegration in a few days to <30% loss of mechanical strength in 40 days. Furthermore, chain extension of PEG macromers with short lactide segments improved vasculogenic expression of MSCs and EPCs encapsulated in the hydrogel.

## Conclusion

In this work, the effect of chemical composition and segment number (n) on gelation characteristics, compressive modulus, and degradation of hydroxy acid-chain-extended star polyethylene glycol acrylate (SPEXA) hydrogels was investigated with incubation time. The hydroxy acid monomers included glycolide (G, least hydrophobic), L-lactide (L), p-dioxanone (D) and -caprolactone (C, most hydrophobic). Chain extension of star PEG macromers with short hydroxy acid segments generated water soluble macromers with faster gelation rates, lower sol fractions, higher compressive moduli, and a wide-ranging degradation times. For all n values, the gelation rate of the more hydrophobic SPELA and SPEDA macromers was significantly faster than those of SPEDA and SPEGA. This was attributed to the formation of micellar structures by the macromers in aqueous solution with hydroxy acid chain-extension and localization of the reactive acrylate groups within the micelles. For a given n value, the extent of micelle formation for SPECA and SPELA macromers was higher than SPEDA and SPEGA, leading to their faster gelation rates. Consistent with the formation of micelles, the compressive modulus of SPEXA gels increased with n. SPEGA gels with the highest fraction of inter-molecular crosslinks had the most increase in compressive modulus with n whereas SPELA and SPECA had the lowest increase in modulus. The swelling ratio of SPEXA gels decreased significantly with increasing n with SPEGA and SEPCA having the highest and lowest swelling ratios, respectively. In the case of SPELA gels, the swelling ratio initially decreased with increasing n in the first 7 day of incubation but the trend was reversed after 7 days. This inversion was attributed to a faster increase in hydrophilicity of SPELA gel with mass loss as n increased. SPEXA gels exhibited a wide range of degradation times from a few days for SPEGA to a few weeks for SPELA, a few months for SPEDA, and many months for SPECA. Further, when marrow stromal cells (MSCs) and endothelial progenitor cells (EPCs) were co-encapsulated in SPEXA gels, the faster degrading SPELA gel compared to SPECA and SPEDA had the highest collagen content and highest expression of vasculogenic markers PECAM-1, VE-cadherin and vWF after 12 days incubation in vasculogenic medium.

## Acknowledgments

This work was supported by research grants to E. Jabbari from the National Science Foundation under grant Nos. DMR1049381 and IIP-1357109, the National Institutes of Health under Grant No. AR063745, the Arbeitsgemeinschaft Fur Osteosynthesefragen (AO) Foundation under Grant No. C10-44J, and the University of South Carolina office of VP for Research under grant no. 15510-14-36182. The authors thank Samaneh K. Sarvestani for assistance with cell cultivation.

## References

1. Seliktar D. Designing cell-compatible hydrogels for biomedical applications. Science. 2012; 336:1124–1128. [PubMed: 22654050]
2. Hoffman MD, Xie C, Zhang XP, Benoit DSW. The effect of mesenchymal stem cells delivered via hydrogel-based tissue engineered periosteum on bone allograft healing. Biomaterials. 2013; 34:8887–8898. [PubMed: 23958029]
3. Moshaverinia A, Chen CD, Akiyama K, Xu XT, Chee WWL, Schricker SR, Shi ST. Encapsulated dental-derived mesenchymal stem cells in an injectable and biodegradable scaffold for applications in bone tissue engineering. J Biomed Mater Res Part A. 2013; 101:3285–3294.
4. Lei YG, Schaffer DV. A fully defined and scalable 3D culture system for human pluripotent stem cell expansion and differentiation. Proc Natl Acad Sci U S A. 2013; 110:E5039–E5048. [PubMed: 24248365]
5. Peppas, NA.; Lustig, SR. hydrogels in medicine and pharmacy. I. Fundamentals. CRC Press; Boca Raton, FL: 2004. solute diffusion in hydrophilic network structures.
6. Nicodemus GD, Bryant SJ. Cell encapsulation in biodegradable hydrogels for tissue engineering applications. Tissue Eng Part B Rev. 2008; 14:149–165. [PubMed: 18498217]
7. Liu SQ, Tay R, Khan M, Ee PLR, Hedrick JL, Yang YY. Synthetic hydrogels for controlled stem cell differentiation. Soft Matter. 2010; 6:67–81.
8. Cushing MC, Anseth KS. Hydrogel cell cultures. Science. 2007; 316:1133–1134. [PubMed: 17525324]
9. Zhu JM. Bioactive modification of poly(ethylene glycol) hydrogels for tissue engineering. Biomaterials. 2010; 31:4639–4656. [PubMed: 20303169]
10. He X, Yang X, Jabbari E. Combined effect of osteopontin and BMP-2 derived peptides grafted to an adhesive hydrogel on osteogenic and vasculogenic differentiation of marrow stromal cells. Langmuir. 2012; 28:5387–5397. [PubMed: 22372823]
11. He X, Ma J, Jabbari E. Effect of grafting RGD and BMP-2 protein-derived peptides to a hydrogel substrate on osteogenic differentiation of marrow stromal cells. Langmuir. 2008; 24:12508–12516. [PubMed: 18837524]
12. Adeloew C, Segura T, Hubbell JA, Frey P. The effect of enzymatically degradable poly(ethylene glycol) hydrogels on smooth muscle cell phenotype. Biomaterials. 2008; 29:314–326. [PubMed: 17953986]
13. Nair LS, Laurencin CT. Biodegradable polymers as biomaterials. Prog Polym Sci. 2007; 32:762–798.
14. Moeinzadeh S, Barati D, He X, Jabbari E. Gelation characteristics and osteogenic differentiation of stromal cells in inert hydrolytically degradable micellar polyethylene glycol hydrogels. Biomacromolecules. 2012; 13:2073–2086. [PubMed: 22642902]
15. Moeinzadeh S, Khorasani SN, Ma J, He X, Jabbari E. Synthesis and gelation characteristics of photo-crosslinkable star Poly (ethylene oxide-co-lactide-glycolide acrylate) macromonomers. Polymer. 2011; 52:3887–3896. [PubMed: 21927508]
16. Moeinzadeh S, Barati D, Sarvestani SK, Karaman O, Jabbari E. Nanostructure formation and transition from surface to bulk degradation in polyethylene glycol gels chain-extended with short hydroxy acid segments. Biomacromolecules. 2013; 14:2917–2928. [PubMed: 23859006]
17. Moeinzadeh S, Jabbari E. Mesoscale simulation of the effect of a lactide segment on the nanostructure of star poly(ethylene glycol-co-lactide)-acrylate macromonomers in aqueous solution. J Phys Chem B. 2012; 116:1536–1543. [PubMed: 22236036]

18. Khetan S, Guvendiren M, Legant WR, Cohen DM, Chen CS, Burdick JA. Degradation-mediated cellular traction directs stem cell fate in covalently crosslinked three-dimensional hydrogels. Nature Mater. 2013; 12:458–465. [PubMed: 23524375]
19. Boontheekul T, Hill EE, Kong HJ, Mooney DJ. Regulating myoblast phenotype through controlled gel stiffness and degradation. Tissue Eng. 2007; 13:1431–1442. [PubMed: 17561804]
20. Chatterjee K, Lin-Gibson S, Wallace WE, Parekh SH, Lee YJ, Cicerone MT, Young MF, Simon CG. The effect of 3D hydrogel scaffold modulus on osteoblast differentiation and mineralization revealed by combinatorial screening. Biomaterials. 2010; 31:5051–5062. [PubMed: 20378163]
21. Chen YC, Lin RZ, Qi H, Yang YZ, Bae HJ, Melero-Martin JM, Khademhosseini A. Functional human vascular network generated in photocrosslinkable gelatin methacrylate hydrogels. Adv Func Mater. 2012; 22:2027–2039.
22. Henderson JA, He X, Jabbari E. Concurrent differentiation of marrow stromal cells to osteogenic and vasculogenic lineages. Macromol Biosci. 2008; 8:499–507. [PubMed: 17941111]
23. He X, Jabbari E. Material properties and cytocompatibility of injectable MMP degradable poly(lactide ethylene oxide fumarate) hydrogel as a carrier for marrow stromal cells. Biomacromolecules. 2007; 8:780–792. [PubMed: 17295540]
24. Yang X, Sarvestani SK, Moeinzadeh S, He X, Jabbari E. Three-dimensional-engineered matrix to study cancer stem cells and tumorsphere formation: effect of matrix modulus. Tissue Eng Part A. 2013; 19:669–684. [PubMed: 23013450]
25. Sarvestani AS, Xu W, He X, Jabbari E. Gelation and degradation characteristics of in situ photo-crosslinked poly(L-lactid-co-ethylene oxide-co-fumarate) hydrogels. Polymer. 2007; 48:7113–7120.
26. Ma J, He X, Jabbari E. Osteogenic differentiation of marrow stromal cells on random and aligned electrospun poly(L-lactide) nanofibers. Ann Biomed Eng. 2011; 39:14–25. [PubMed: 20577811]
27. Kahler CM, Wechselberger J, Hilbe W, Gschwendtner A, Colleselli D, Niederegger H, Boneberg EM, Spizzo G, Wendel A, Gunsilius E, Patsch JR, Hamacher J. Peripheral infusion of rat bone marrow derived endothelial progenitor cells leads to homing in acute lung injury. Respiratory Res. 2007; 8:1–17.
28. Yang NN, Li DW, Jiao P, Chen B, Yao ST, Sang H, Yang MF, Han JJ, Zhang Y, Qin SC. The characteristics of endothelial progenitor cells derived from mononuclear cells of rat bone marrow in different culture conditions. Cytotechnology. 2011; 63:217–226. [PubMed: 21331655]
29. Ghajar CM, Kachgal S, Kniazeva E, Mori H, Costes SV, George SC, Putnam AJ. Mesenchymal cells stimulate capillary morphogenesis via distinct proteolytic mechanisms. Exp Cell Res. 2010; 316:813–825. [PubMed: 20067788]
30. Rao RR, Peterson AW, Ceccarelli J, Putnam AJ, Stegemann JP. Matrix composition regulates three-dimensional network formation by endothelial cells and mesenchymal stem cells in collagen/fibrin materials. Angiogenesis. 2012; 15:253–264. [PubMed: 22382584]
31. Chen KL, Sahoo S, He PF, Ng KS, Toh SL, Goh JCH. A hybrid silk/RADA-based fibrous scaffold with triple hierarchy for ligament regeneration. Tissue Eng Part A. 2012; 18:1399–1409. [PubMed: 22429111]
32. Jabbari E, He X, Valarmathi MT, Sarvestani AS, Xu W. Material properties and bone marrow stromal cells response to in situ crosslinkable RGD-functionlized lactide-co-glycolide scaffolds. J Biomed Mater Res Part A. 2009; 89A:124–137.
33. Kiran MS, Viji RI, Kumar SV, Prabhakaran AA, Sudhakaran PR. Changes in expression of VE-cadherin and MMPa in endothelial cells: Implications for angiogenesis. Vascular Cell. 2011; 36:1–12. [PubMed: 21349158]
34. Pfaffl MW. A new mathematical model for relative quantification in real-time RT-PCR. Nucleic Acids Res. 2001; 29:e45. [PubMed: 11328886]
35. Cima LG, Lopina ST. Network structures of radiation-cross-linked star polymer gels. Macromolecules. 1995; 28:6787–6794.
36. Sanson N, Rieger J. Synthesis of nanogels/microgels by conventional and controlled radical crosslinking copolymerization. Polym Chem. 2010; 1:965–977.
37. Flory, PJ. Principles of Polymer Chemistry. Cornell University Press; New York: 1953.

38. Elliott JE, Bowman CN. Kinetics of primary cyclization reactions in cross-linked polymers: an analytical and numerical approach to heterogeneity in network formation. Macromolecules. 1999; 32:8621–8628.
39. Li ZL, Dormidontova EE. Equilibrium chain exchange kinetics in block copolymer micelle solutions by dissipative particle dynamics simulations. Soft Matter. 2011; 7:4179–4188.
40. Nicolai T, Colombani O, Chassenieux C. Dynamic polymeric micelles versus frozen nanoparticles formed by block copolymers. Soft Matter. 2010; 6:3111–3118.
41. Metters AT, Anseth KS, Bowman CN. Fundamental studies of a novel, biodegradable PEG-b-PLA hydrogel. Polymer. 2000; 41:3993–4004.
42. Martens P, Metters AT, Anseth KS, Bowman CN. A generalized bulk-degradation model for hydrogel networks formed from multivinyl cross-linking molecules. J Phys Chem B. 2001; 105:5131–5138.
43. Martens PJ, Bowman CN, Anseth KS. Degradable networks formed from multi-functional poly(vinyl alcohol) macromers: comparison of results from a generalized bulk-degradation model for polymer networks and experimental data. Polymer. 2004; 45:3377–3387.
44. Tsigkou O, Pomerantseva I, Spencer JA, Redondo PA, Hart AR, O'Doherty E, Lin YF, Friedrich CC, Daheron L, Lin CP, Sundback CA, Vacanti JP, Neville C. Engineered vascularized bone grafts. Proc Natl Acad Sci U S A. 2010; 107:3311–3316. [PubMed: 20133604]
45. Levenberg S, Rouwkema J, Macdonald M, Garfein ES, Kohane DS, Darland DC, Marini R, van Blitterswijk CA, Mulligan RC, D'Amore PA, Langer R. Engineering vascularized skeletal muscle tissue. Nature Biotech. 2005; 23:879–884.
46. Bryant SJ, Anseth KS. Hydrogel properties influence ECM production by chondrocytes photoencapsulated in poly(ethylene glycol) hydrogels. J Biomed Mater Res. 2002; 59:63–72. [PubMed: 11745538]
47. Bryant SJ, Anseth KS. Controlling the spatial distribution of ECM components in degradable PEG hydrogels for tissue engineering cartilage. J Biomed Mater Res Part A. 2003; 64A:70–79.
48. Albelda SM, Muller WA, Buck CA, Newman PJ. Molecular and cellular properties of PECAM-1 (endocam/CDF31) - a novel vascular cell cell-adhesion molecule. J Cell Biol. 1991; 114:1059–1068. [PubMed: 1874786]
49. Bautch VL, Redick SD, Scalia A, Harmaty M, Carmeliet P, Rapoport R. Characterization of the vasculogenic block in the absence of vascular endothelial growth factor-A. Blood. 2000; 95:1979–1987. [PubMed: 10706864]
50. Sadler JE. Biochemistry and genetics of von Willebrand factor. Ann Rev Biochem. 1998; 67:395–424. [PubMed: 9759493]

- Hydrogels based on hydroxy acid-chain-extended star polyethylene glycol acrylate (SPEXA) macromers are synthesized.
- Chain-extension with hydroxyl acids generated hydrogels with faster gelation, lower sol fraction, and higher compressive modulus.
- SPEXA gels exhibit a wide range of degradation times from a few days to many months.
- SPEXA gels with L-lactide as the hydroxyl acid exhibited a 10-day delayed swelling response in aqueous medium.
- Marrow stromal cells and endothelial progenitor cells show highest expression of vasculogenic markers and highest collagen content when co-encapsulated in the SPEXA gel with fast-degrading lactide segments.

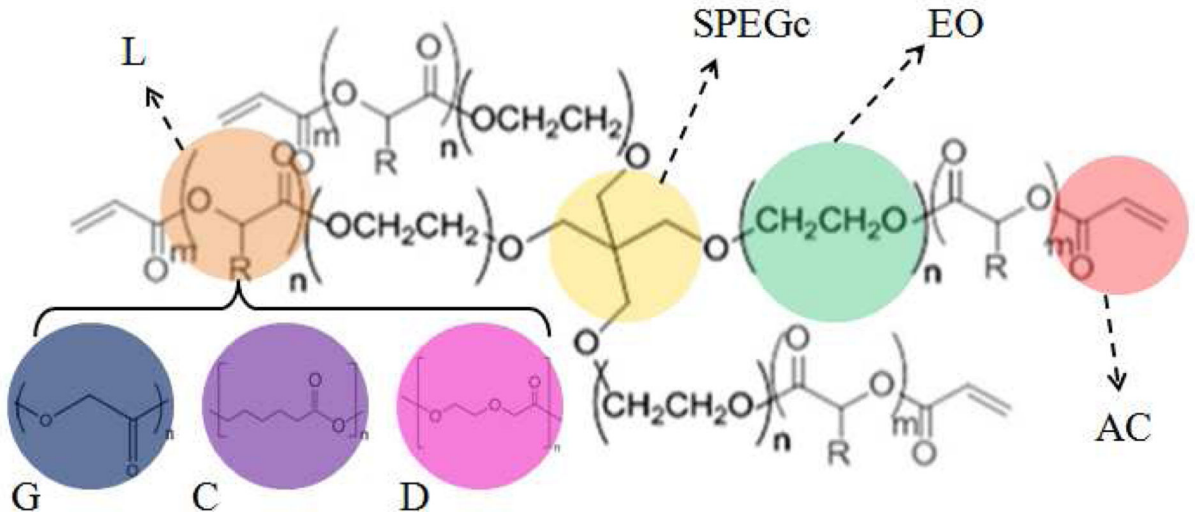


**Figure 1.**

Schematic representation for the chemical composition of SPEXA macromers. Ethylene oxide (EO) repeat units, SPEG core (SPEGc) and acrylate (AC) functional groups are shown by green, yellow and light red, respectively. Chain extensions with short lactide (L), glycolide (G), p-dioxanone (D) and -caprolactone(C) are shown by brown, blue, pink and purple colors, respectively.

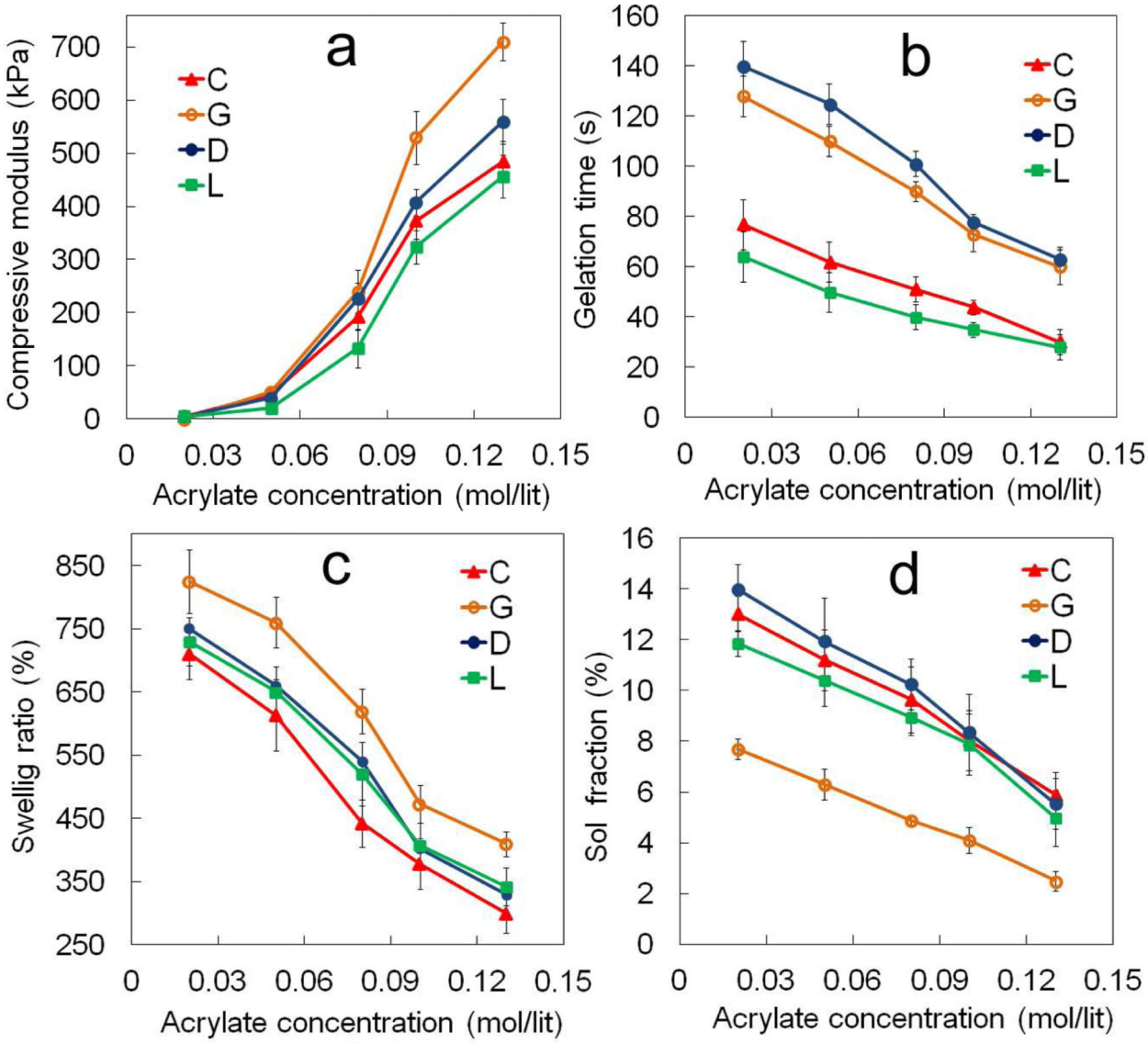


**Figure 2.**

Effect of acrylate concentration in SPEXA hydrogel precursor solution on (a) compressive modulus, (b) gelation time, (c) swelling ratio and (d) sol fraction of SPEXA hydrogels. Error bars correspond to means ± 1 SD for n=3.

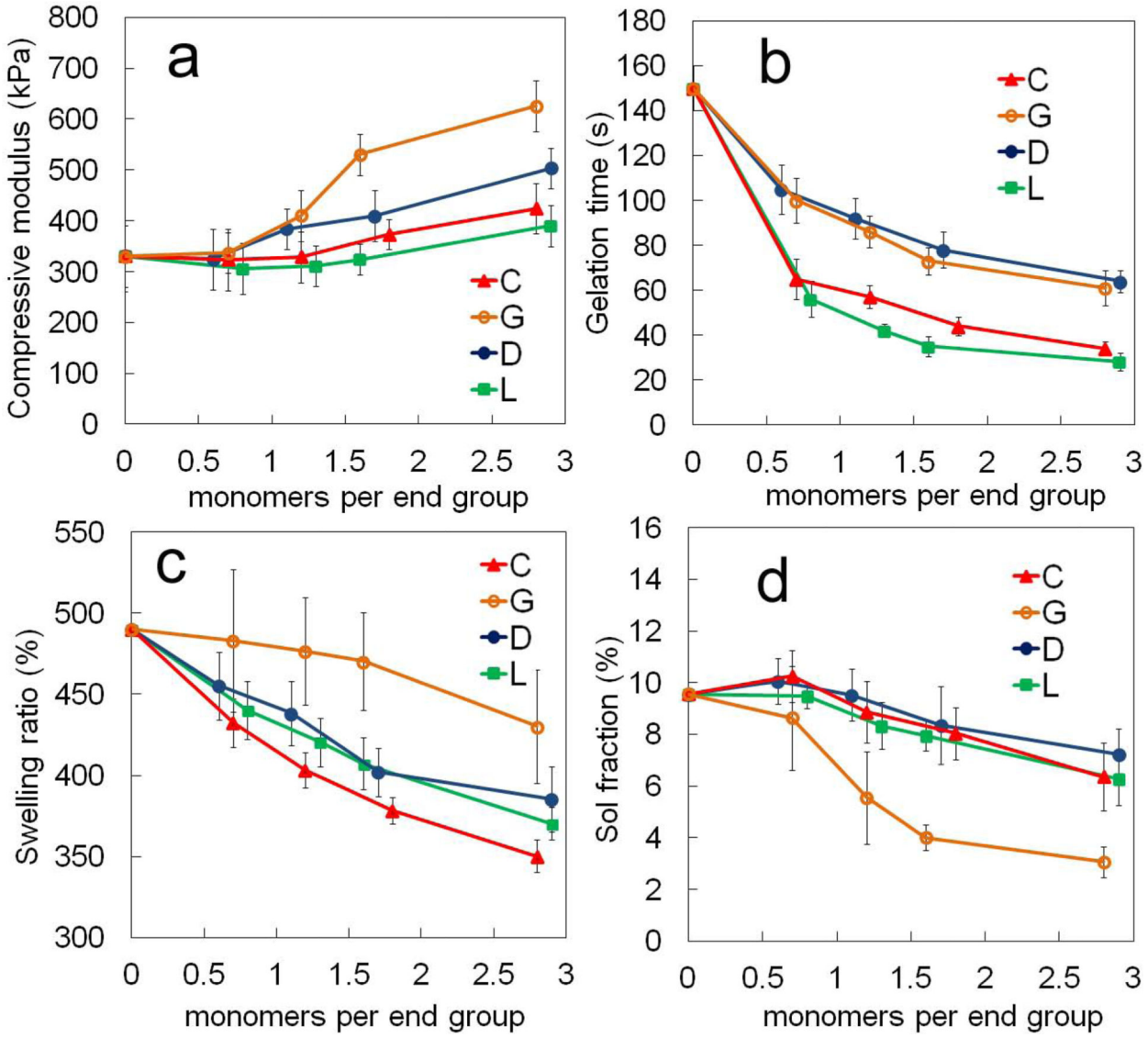


**Figure 3.**

Effect of number of monomers in the short hydroxy acid segment on each macromer arm on (a) compressive modulus, (b) gelation time, (c) swelling ratio and (d) sol fraction of SPEXA hydrogels. Error bars correspond to means ± 1 SD for n=3.

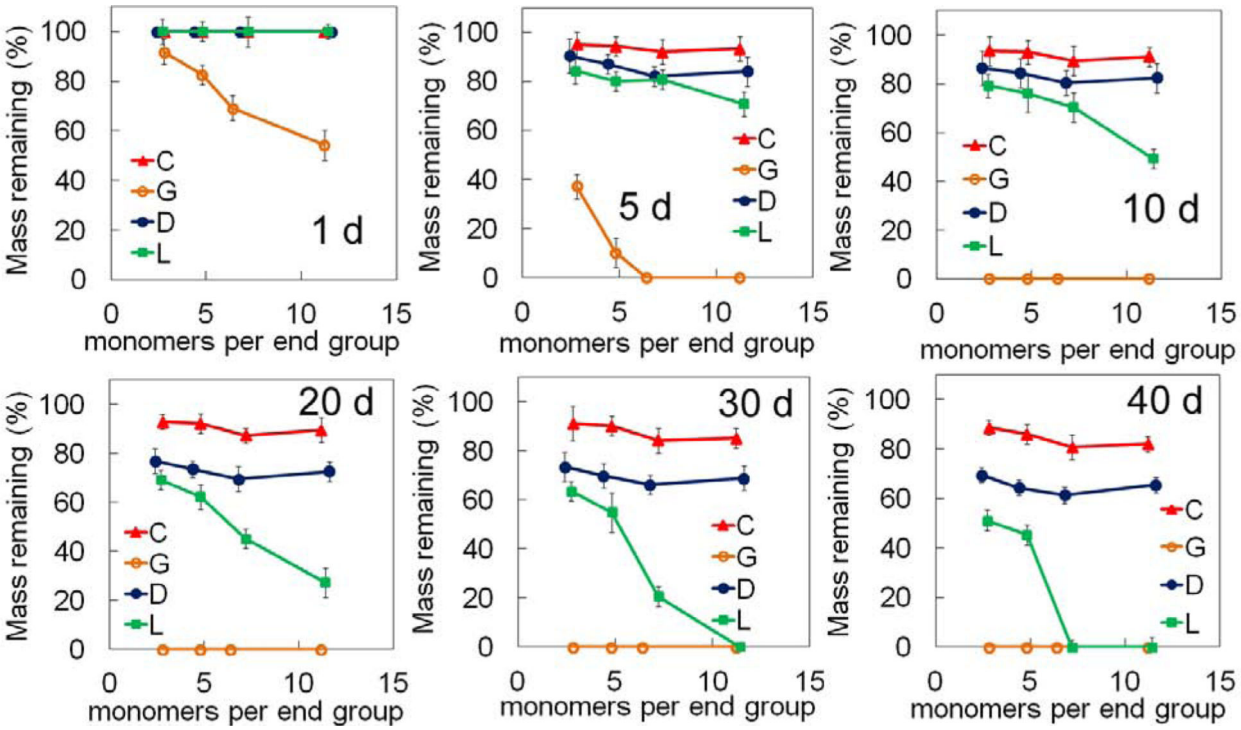


**Figure 4.**

Effect of number of monomers in the short hydroxy acid segment on each macromer arm on the remaining mass of SPEXA hydrogels with incubation time in basal culture medium without FBS. Error bars correspond to means ± 1 SD for n=3.

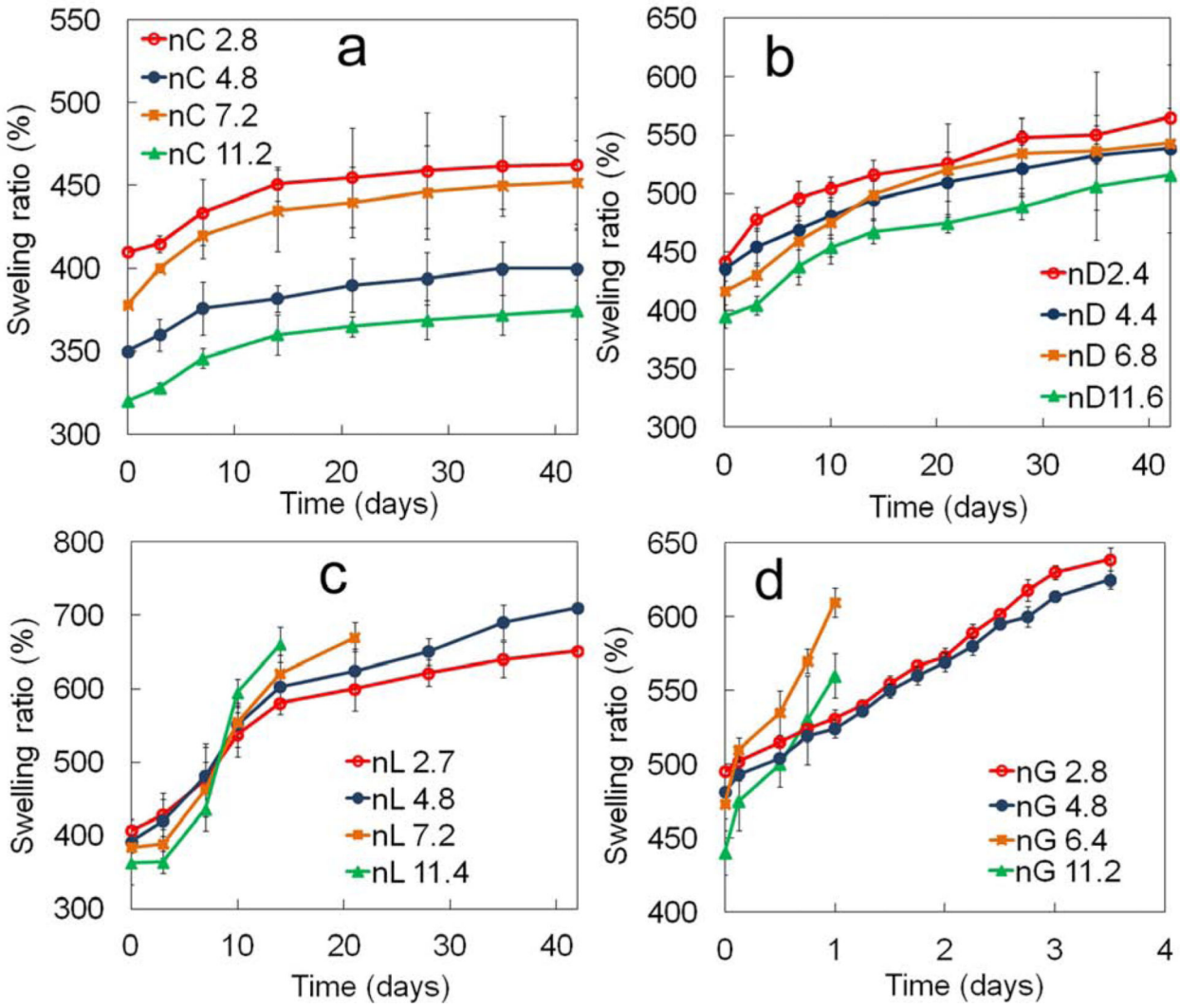


**Figure 5.**

Effect of number of monomers in the short hydroxy acid segment on each macromer arm on swelling ratio with incubation time for (a) SPECA, (b) SPEDA, (c) SPELA and (D) SPEGA hydrogels. Error bars correspond to means ± 1 SD for n=3.

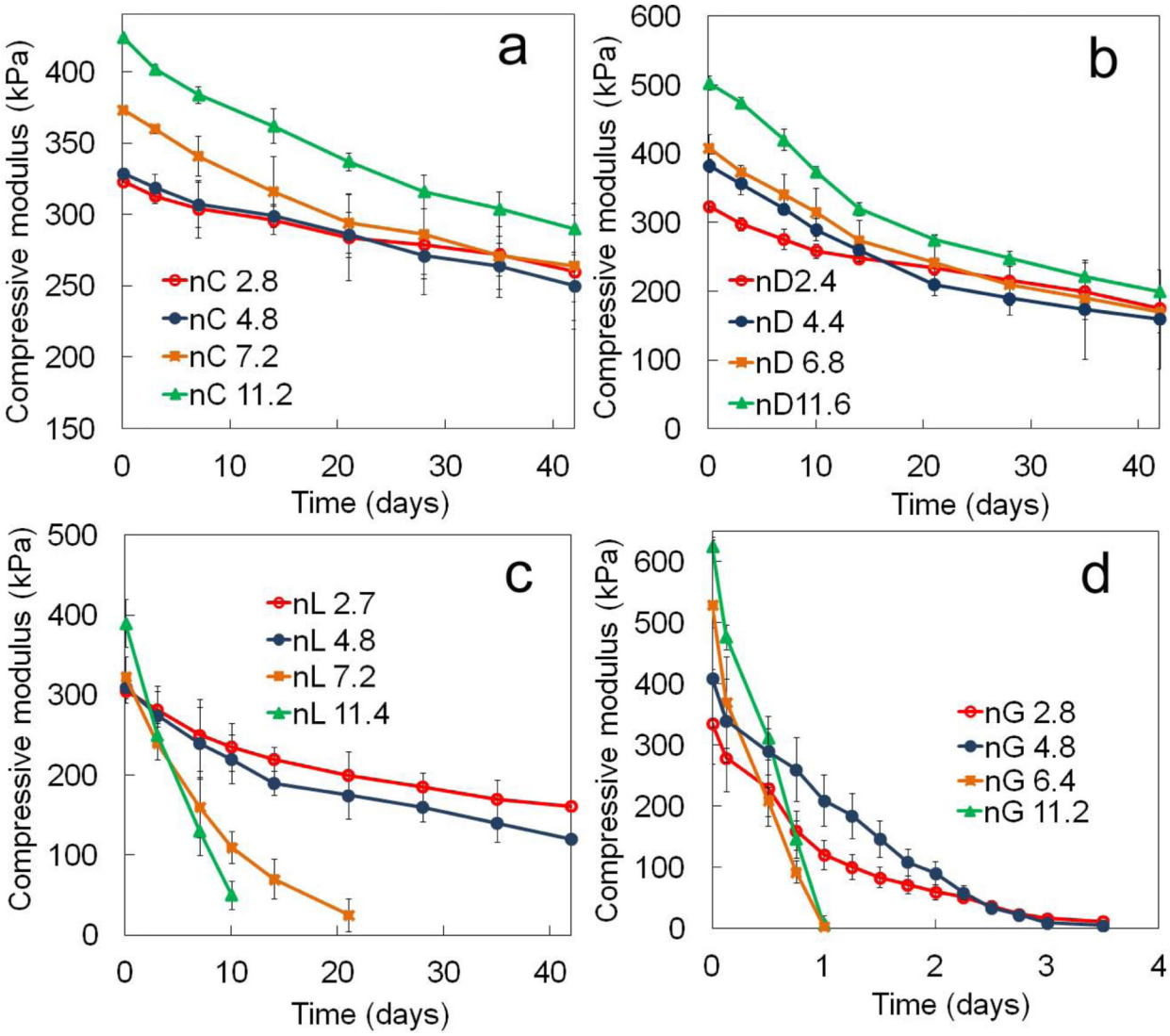


**Figure 6.**

Effect of number of monomers in the short hydroxy acid segment on each macromer on compressive modulus with incubation time for (a) SPECA, (b) SPEDA, (c) SPELA and (D) SPEGA hydrogels. Error bars correspond to means ± 1 SD for n=3.

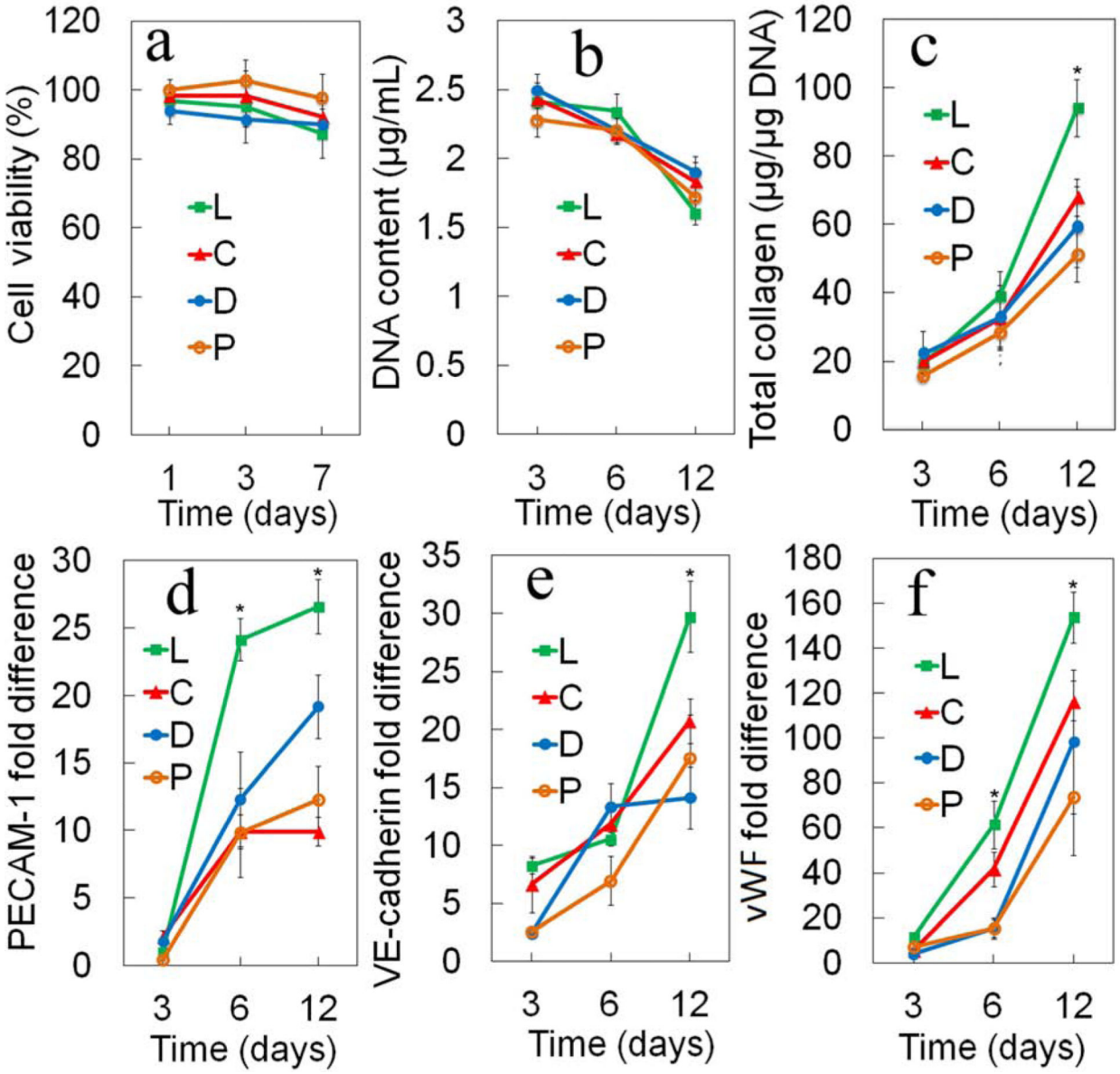


**Figure 7.**

(a) Cell viability (b) DNA content, (c) total collagen content, mRNA expression levels of Pecam-1 (d), VE-cadherin(e) and vWF (f) for MSC/EPCs encapsulated in SPELA (L), SPEDA (D), SPECA(C) and PEGDA (P) hydrogels with incubation time in vasculogenic medium. One star indicates a statistically significant difference between the test group and all other groups at the same time point. Error bars correspond to means 1 SD for n=3.

**Table 1**

Number of hydroxy acid monomers per macromer (nX), number average molecular weight ($M_n$ ), monomer to PEG molar feed ratio, average number of hydroxy acid monomers per macromer arm, and average number of acrylates per macromere arm for SPEXA macromers.

| Macromonomer | $\bar{Mn}$ (±100) | Monomer/PEG feed molar ratio | monomers per end group (±0.1) | acrylates per end group (±0.05) |
|---|---|---|---|---|
| SPEXA-nX0 | 5300 | 0 | 0 | 0.85 |
| SPECA-nC2.8 | 5500 | 5 | 0.7 | 0.85 |
| SPECA-nC4.8 | 5700 | 7.5 | 1.2 | 0.81 |
| SPECA-nC7.2 | 6000 | 10 | 1.8 | 0.78 |
| SPECA-nC11.2 | 6400 | 15 | 2.8 | 0.75 |
| SPEDA-nD2.4 | 5400 | 5 | 0.6 | 0.82 |
| SPEDA-nD4.4 | 5600 | 7.5 | 1.1 | 0.79 |
| SPEDA-nD6.8 | 5900 | 10 | 1.7 | 0.75 |
| SPEDA-nD11.6 | 6300 | 15 | 2.9 | 0.73 |
| SPEGA-nG2.4 | 5600 | 5 | 0.8 | 0.87 |
| SPEGA-nG4.4 | 5700 | 7.5 | 1.2 | 0.82 |
| SPEGA-nG6.4 | 5900 | 10 | 1.6 | 0.81 |
| SPEGA-nG11.2 | 6500 | 15 | 2.8 | 0.78 |
| SPELA-nL3.2 | 5700 | 5 | 0.8 | 0.86 |
| SPELA-nL4.4 | 5800 | 7.5 | 1.1 | 0.83 |
| SPELA-nL6.4 | 6200 | 10 | 1.6 | 0.82 |
| SPELA-nL11.6 | 6900 | 15 | 2.9 | 0.74 |
| LPELA-nL3.6 | 5200 | 5 | 1.8 | 0.85 |
| LPELA-nL7.4 | 5800 | 10 | 3.7 | 0.87 |
| LPELA-nL9.6 | 6100 | 15 | 4.8 | 0.77 |
| LPELA-nL14.8 | 6800 | 20 | 7.4 | 0.71 |